Case Studies in Construction Materials 17 (2022) e01465

Contents lists available at ScienceDirect

Case Studies in Construction Materials

journal homepage: www.elsevier.com/locate/cscm

Case study

Study on laboratory and engineering application of multi source solid waste based soft soil solidification materials

Benan Shu [a,*], Weizhong Chen [b], Tengyu Yang [a], Zhirong Xie [b], Yanfei Ren [a], Yongling Li [a], Lishang Zheng [a], Guodong Zeng [a], Menglin Li [c], Diego Maria Barbieri [d]

[a] *Foshan Transportation Science and Technology Co., Ltd, Foshan 528000, China*
[b] *Foshan Jianying Development Co., Ltd, Foshan 528000, China*
[c] *State Key Laboratory of Silicate Materials for Architectures, Wuhan University of Technology, Wuhan 430000, China*
[d] *Department of Civil and Environmental Engineering, Norwegian University of Science and Technology, Trondheim, Norway*

A R T I C L E I N F O

Keywords:
Solidification
Sodium sulfate
Solid waste
Unconfined compressive strength
Deep mixing pile

A B S T R A C T

The study on multi source solid wastes solidified organic clay is limited, as well as engineering application in deep mixing pile. In this paper, steel slag powder (SS) and high calcium fly ash (HCFA) are used as raw materials, by-product sodium sulfate was recycled to develop a kind of multi-source solid waste based low carbon emission solidifying material. The solidification mechanism was analyzed by scanning electron microscope (SEM), X-ray diffraction (XRD), thermogravimetry (TG) and pH tests. Finally, the solidifying agent was applied to the deep mixing pile project, and the solidification effect was studied. The results reveal that the fluidity of preferred multi-source solid waste based solidifying agent slurry was 170 mm (50 °C, 1 h), which is 55% higher than that of cement. The optimum content of solidifying agent in organic clay was determined as 27%, and the unconfined compressive strength (28d) of the solidified soil was 5 MPa. Na_2SO_4 showed double effect of alkali activation and dense packing. The pH of solidifying agent slurry was maintained at 13.31 after the addition of 0.7% Na_2SO_4. More C-S-H and AFt generated under the effect of pH and SO_4^{2-}. The application study reveals that the multi-source solid waste based solidifying agent deep mixing pile exhibited excellent pile integrity in organic clay. The compressive strength of deep mixing pile with the 40 kg/m solidifying agent at the curing of 14d and 28d is 0.95 MPa and 2.77 MPa, respectively. Solidifying agent deep mixing pile field strength prediction equation "$y = 0.832x + 0.1225$, $R^2 = 0.936$" was proposed.

1. Introduction

With the proposal of "2030 carbon peak, 2060 carbon neutralization" from the government of China, it has become a consensus to reduce carbon emission through technological innovation [1,2]. Cement production is one of the high carbon emission industries. Thus it has become a trend to make full use of solid waste to replace cement by technological innovation [3,4].

Cement deep mixing pile is widely used in soft foundation reinforcement because of its excellent economy and simple operation [5]. Humus acid in organic matter could destroy the hydration structure, which make it difficult for cement to bond soil particles during soft soil solidification [6,7]. Synchronously, the high water content also weakens the solidifying effect of cement. Therefore, cement

* Corresponding author.
E-mail address: shuba@whut.edu.cn (B. Shu).

https://doi.org/10.1016/j.cscm.2022.e01465
Received 25 July 2022; Received in revised form 27 August 2022; Accepted 4 September 2022
Available online 6 September 2022
2214-5095/

deep mixing piles in organic clay commonly showed poor integrity and low strength [8–11].

Currently, it has become a hot research direction to recycling solid wastes with pozzolanic activity to solidify soft soil based on alkali activation technology. Compared with cement production, there is a 60%– 80% CO_2 emission reduction for alkali-activated cementitious materials [12–14]. Alkali activation process can be divided into three periods: dissolution of Si and Al monomer, monomer reconfiguration and poly-condensation [15]. The solid wastes that can be activated by alkali mainly includes ground granulated blast furnace slag (GGBS), fly ash (FA)and steel slag powder (SS). Alkali activators are mainly sodium silicate, sodium carbonate, sodium hydroxide, potassium hydroxide and calcium hydroxide [16–18]. Shu et al. [19] studied the effects of different types of activators on the properties of steel slag solidified organic clay. It can be observed that the UCS of solidified soil is significantly improved to 2.37 MPa when 10% sodium hydroxide and 10% sodium carbonate are incorporated. Goodarzi et al. [20] revealed that the alkali activated slag can be used to solidify the clay contaminating with Zn. Compared with cement, MgO showed the stronger activation effect on GGBS. He et al. [21] indicated that GGBS had better solidification effect than soda residue and carbide slag. The higher strength of solidified soil mainly attributes to the pore filling effect of ettringite.

However, the alkali activator corrodes metal equipment, as well as poses a serious threat to human skin during the process of production and construction. In addition, excessive utilization of alkali activators also can destroy the acid-base balance of soil [22]. In view of this, more studies focus on the cleaner activators, such as nano-particles and Na_2SO_4. Bahmani et al. [23] found that the addition of 0.5% nano-SiO_2 significantly improved the mechanical property of solidified residual soil. The smaller size of nano-silica, the better solidification effect on residual soil. Jia et al. [24] demonstrated that the synergistic effect of desulfurized ash and steel slag powder can be used to solidify silt soil. Chen et al. [25] demonstrated that the addition of Na_2SO_4 improved the strength of solidified granulated copper slag.

For each ton of viscose fiber, nearly 300 m^3 of wastewater is discharged during the production, and the sulfate concentration in the wastewater is approximately 30,000 ppm. In 2021, 61.524 million tons of synthetic fiber was produced in China. Therefore, tens of billions cubic meters of wastewater have been produced. A large amount of by-product sodium sulfate is produced, however which has not been effectively recycled [26,27]. With the rapid development of China's economy, the accumulation quantities of fly ash (FA) are about 2.5 billion tons, and the annual production of steel slag in China is about 180 million tons, and the utilization rate is less than 20% [28]. The massive no-recycled FA and SS cause serious resource waste, land occupation and groundwater pollution. Meanwhile, the study on multi source solid wastes solidified organic clay is limited, as well as application on deep mixing piles.

In view of this, industrial solid wastes, which includes high calcium fly ash (HCFA) and steel slag powder (SS) were used as raw materials, Na_2SO_4, a by-product from chemical fiber industry, was used as activator to prepare the solidifying agent. The optimal proportion was optimized. Then, the solidification mechanism was studied. Finally, the application research of the solidifying agent in deep mixing pile project was carried out. The improvement effect of the solidifying agent on the integrity and strength of deep mixing pile was analyzed, and the strength prediction was proposed. The multi-source solid waste solidifying agent developed in this work is a kind of cleaner soft soil solidifying material, which can effectively improve the recycling rate of HCFA, SS and by-product Na_2SO_4. In addition, the significant reduction of cement demand in soft foundation consolidation engineering can significantly reduce carbon emissions. This research accelerates to realize the strategic goal of "2030 carbon peak, 2060 carbon neutralization".

2. Materials and methods

2.1. Materials

2.1.1. Organic clay

The organic clay used in this work is drilled out at depth of − 15 m (as shown in Fig. 1a and b). The core sample is firstly dried at 60 °C, and then the dried core sample is ground and screened by 2 mm sieve to obtain the experiment sample (as shown in Fig. 1c). The

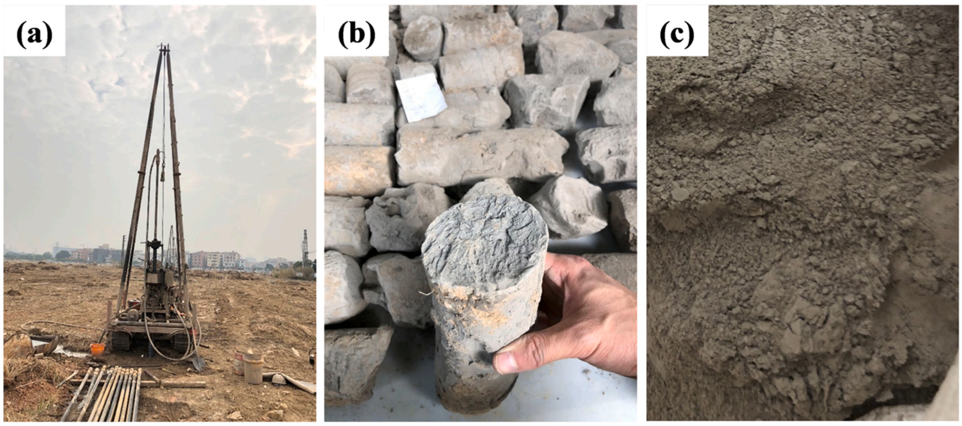

Fig. 1. Acquisition process of organic clay sample: (a) field drilling, (b) dried organic clay core sample, (c) screened organic clay.

geotechnical test is carried out, and the basic parameters are shown in Table 1. The experiment soil belongs to organic clay with the feature of high content water and organic matter. The contents of natural water and organic matter are 68.3% and 7.32%, respectively.

2.1.2. *Multi-source solid wastes*

Multi-sources solid wastes are shown in Fig. 2. The SS (as shown in Fig. 2b) is purchased from Guangdong Province Shaoguan Steel Group Co., Ltd. The HCFA (as shown in Fig. 2a) is obtained from Foshan Sanshui Hengyi Thermal Power Co., Ltd. The specific surface area and average particle size of SS and HCFA are 405 m^2/kg and 48 μm, 435 m^2/g and 44 μm, respectively. The activity indexes of SS and HCFA are 68% and 81% respectively. The main components of these two kinds of mineral admixtures are shown in Table 2.

Na_2SO_4, the industrial by-product used in this work (as shown in Fig. 2c), is obtained from Guangzhou Lanjing Chemical Fiber Co., Ltd. The chemical composition is tested, and the results are shown in Table 3. The PO 42.5 Portland cement is purchased from China Resources Cement (Foshan) Co., Ltd. The initial and final setting time of the cement are 130 min and 170 min, respectively. The compressive strength after curing for 28 days is 48.3 MPa.

2.2. *Experimental methods*

2.2.1. *Laboratory test of solidified soil*

The stirring, molding, curing and strength tests process of the solidified soil are conducted according to the specification of "mix proportion design of cement soil" (JGJ/T 233–2011). Firstly, the weighed components and dried soil are poured into a pot, and stirred for one minute. Then, a certain amount of water is added, and stirred for 2 min at300rpm, and then continually 3 min at 1000 rpm. The slurry is poured into a mold with the diameter of 50 mm and the height of 100 mm (as shown in Fig. 3a). The mold with slurry is vibrated for 2 min, then covered with fresh-keeping film, and cured at 20 °C for 48 h (as shown in Fig. 3b). After de-mold, the cylinder solidified soil test block is placed in the curing room for standard curing (as shown in Fig. 3c). The unconfined compressive strength (UCS) of solidified soil is conducted on the machine (manufactured by Suzhou Yuchuang Fluid Technology Co., Ltd), and the loading rate of force is set at 80 N/s (as shown in Fig. 3d).

2.2.2. *Microscopic test*

Scanning electron microscope (SEM) test is operated on the machine JSM-7500 F, and the resolution of backscattered electron image and secondary electron resolution are 1.5 nm and 1.0 nm, respectively. Magnification is determined as 1000x, 2000x, 5000x and 10000x. The sample is sprayed with gold before SEM test. Thermo-gravimetric (TG) test is conducted on the machine STA449F3 (NETZSCH, Germany). The temperature accuracy is ± 1.5 °C. The heating rate and temperature range used in this work are 10 °C and 30–800 °C, respectively.

X-ray diffraction (XRD) test is operated on the machine Empyrean (PANalytical B.V, Netherlands). The power of high voltage generator is 4kw, and the maximum high voltage and maximum anode current are 60 kV and 60 mA, respectively. The range of diffraction angles tested in this work is 10–80°.

2.2.3. *Engineering application*

The determined solidifying agent is applied in two projects, that are, Shunde District "robot valley" and "Longxiang bridge". The construction process is shown in Fig. 4. The slurry system exhibited in Fig. 4a includes powder feeding, weighting and mixing, slurry storage and pumping. The specific gravity of the slurry is tested before grouting, as shown in Fig. 4b. Fig. 4c shows the construction process of deep mixing pile. The content of grouted slurry is controlled by frequency. Four times of mixing is applied. A large number of white sulfate crystals can be observed on the surface of the mixing pile after several days of curing, as shown in Fig. 4d. The deep mixing pile is drilled at specific curing time, as shown in Fig. 4e.

3. Results and discussion

3.1. *Properties of solidifying agent*

3.1.1. *Optimum of the solidifying agent*

Based former study [19], the follow nine groups of mix proportions are proposed, as shown in Table 4. It can be found that the addition of by -product Na_2SO_4 significantly improved the strength of solidified soil. Under the condition of constant content of A (self-developed high activity calcium based oxide) and sodium sulfate, the strength of solidified soil is positively proportional to the relative content of HCFA, and inversely proportional to the relative content of SS. The reason is that the activity index of HCFA is larger than that of SS, so the content increase of HCFA is more conducive to the strength improvement of solidified soil. The UCS of solidified soil with reasonable content by-product sodium sulfate was nearly 10 times larger than that of the solidified soil without by-product

Table 1
Geotechnical properties of the silt soil.

Geotechnical parameters	Natural water content /%	Organic matter content /%	Dry density, g/ cm^3	Liquid limit /%	Plastic limit /%	< 0.075 mm,%	USCS soil classification
Test result	68.3	7.32	1.54	48.85	27.67	54.5	OH

Fig. 2. Multi- source solid wastes: (a) HCFA, (b) SS and (c) sodium sulfate recovered from the waste liquid in chemical fiber industry.

Table 2
Main components of the two kinds of mineral admixture.

Components	CaO	SiO_2	Al_2O_3	MgO	Fe_2O_3	SO_3
SS	36.8	35.57	12.32	9.08	5.1	0.23
HCFA	40.61	38.31	10.32	1.27	0.37	8.50

Table 3
Performance of Industrial by-product Na_2SO_4.

Parameter	Appearance	Purity /%	Moisture content/%	Iron content/%	Magnesium content/%	Whiteness (R457,%)	pH
Test result	Yellow crystalline	98.6	0.06	0.0044	$<$ 0.01	67.9	6.6

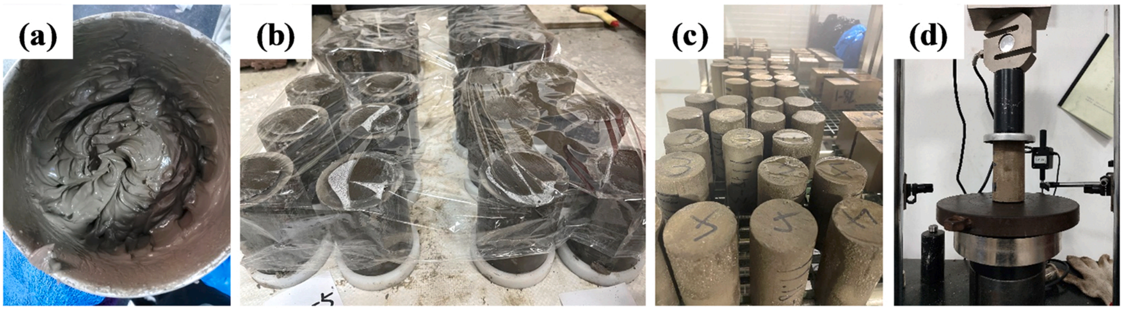

Fig. 3. Laboratory experiment process of solidified soil: (a) strring, (b) molding, (c) curing and (d) unconfined compressive strength test.

sodium sulfate. The reason is shown in Section 3.2, by-product sodium sulfate showed double effect of alkali activation and dense packing. The experiment from Table 4 also reveals that excessive addition of sodium sulfate could lead to the UCS decrease of the solidified soil. The reason is that excessive formation of AFt leads to destruction of three-dimensional network structure of solidified soil. Considering economy and performance surplus, the optimal proportion of the multi-source solid waste solidifying agent can be determined as, A: HCFA: SS: Na_2SO_4 = 0.05: 7.375: 7.375: 0.2.

The unconfined compressive strength of the solidified soil with the optimized solidifying agent in different curing periods is shown in Fig. 5. With the addition of 15% solidifying agent, the strength of solidified soil increases rapidly in the early stage of curing period. The strength is increased by 160% with the curing period extended from 3d to 28d. With the continuous increase of curing time, the strength of the solidified soil increases slowly.

3.1.2. Comprehensive properties of the solidifying agent

The basic properties of the solidifying agent are tested, and the results are shown in Table 5. It can be seen that all indexes of the solidifying agent meet the specification of “Stabilizer for soft soil” (CJ/T 526–2018, China).

As shown in Fig. 6, the initial and 60 min fluidity of solidifying agent are 270 mm and 210 mm, respectively, which are significantly higher than that of cement. The excellent fluidity makes the solidifying agent easier to pump than cement. Thus, the solidifying agent is more suitable for engineering fields such as deep mixing pile, high-pressure rotary jetting piles and deep surface soil grouting. In addition, the fluidity of the solidifying agent slurry after heating at 50 °C for 1 h is 170 mm, which is 55% higher than that of cement. As a result, the solidifying agent is more suitable for application in high-temperature environment in south China (such as Guangdong Province), which is not prone to pipe plugging.

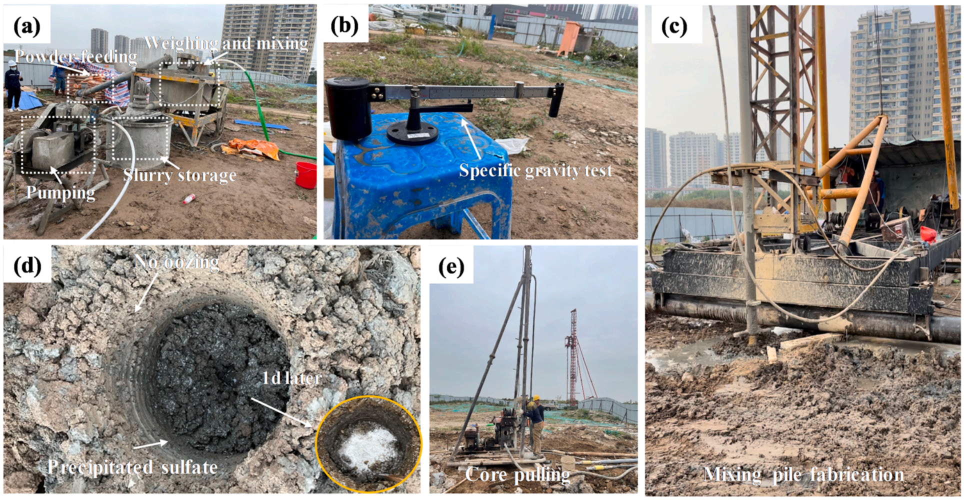

Fig. 4. Construction process of solidifying agent application in deep mixing pile project: (a) pulping system, (b) specific gravity test, (c) deep mixing pile construction, (d) deep mixing pile completed construction and (e) pile core pulling.

Table 4
Mix proportion design of solidifying agent based on orthogonal method.

A/%	HCFA/%	SS/%	Na_2SO_4/%	UCS (28d, MPa)
0.05	9.97	4.98	0	0.38
0.05	7.475	7.475	0	0.28
0.05	4.98	9.97	0	0.21
0.05	7.425	7.425	0.1	3.15
0.05	7.375	7.375	0.2	3.31
0.05	7.325	7.325	0.3	3.07
0.05	9.83	4.92	0.2	3.46
0.05	4.92	9.83	0.2	3.02

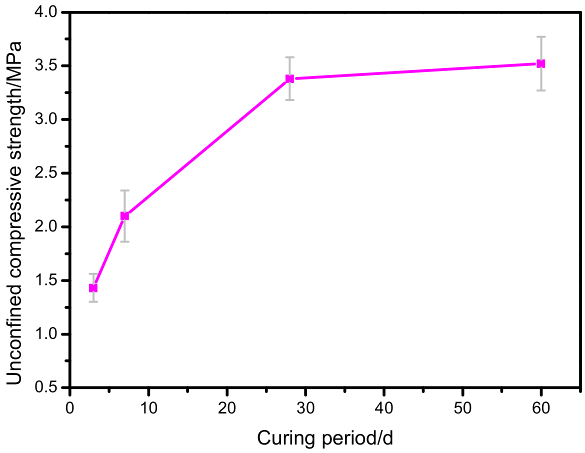

Fig. 5. Unconfined compressive strength of solidified soil at different curing period.

3.1.3. *Effect of content*

The influence of solidifying agent content on the unconfined compressive strength (28d curing age) of solidified organic clay is shown in Fig. 7. It can be found that the strength of solidified soil increases slowly when the content of solidifying agent is at a low level. The strength of solidified soil increases rapidly when the content of solidifying agent is higher than 19%. With the increasing of the content, the strength of the solidified soil increases continuously, and then the strength decreases rapidly. There is an optimal content of the solidifying agent in organic clay, which can be determined as 27%, in which content, the unconfined compressive strength of the solidified soil (28d) was 5 MPa.

Table 5
Basic properties of the solidifying agent.

Performance index		Requirements	Test result
Moisture content/%		≤ 1	0.7
Fineness (sieve residue of square hole with 80 μm)/%		≤ 10	5
Initial setting time/min		≥ 45	150
Fluidity (25 ℃)/s	Initial	≥ 100	270
	30 min	≥ 90	240
	60 min	≥ 80	210

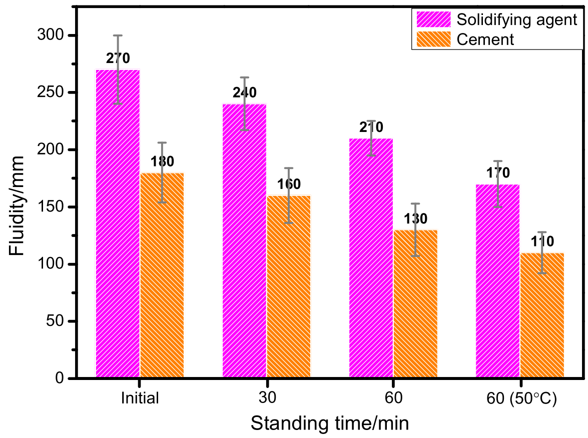

Fig. 6. Fluidity of the solidifying agent at different standing time.

The main reason may be that the organic clay solidification mainly depends on the hydration cementation of the solidifying agent. Therefore, the addition of reasonable content solidifying agent could significantly improve the strength of solidified soil. The integral hydration framework cannot be formed when the content of solidifying agent is at a low level. Therefore, UCS increased slowly. The pore diameter of cement solidified soil is distributed in 300–1000 nm [29]. After the addition of excessive Na_2SO_4, although the pore diameter of solidified soil is tens of times that of cement concrete, excessive large space expansion also can be caused by excessive formation of AFt. The framework structure of solidified soil will be destroyed under the effect of expansion stress. Thus the strength of solidified soil decreased rapidly when the solidifying agent content is higher than 27%.

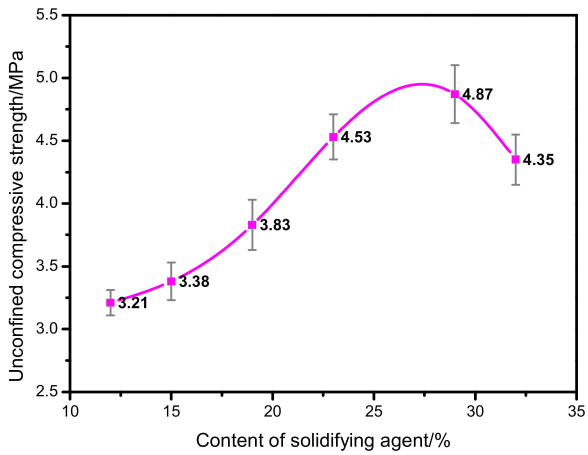

Fig. 7. Unconfined compressive strength of solidified organic clay with different content of solidifying agent.

3.2. Mechanism analysis

3.2.1. Microscopic analysis

3.2.1.1. SEM test. The effect of different content of solidified materials on the micro-morphology of solidified organic clay is shown in Fig. 8. It can be found that the hydration products of solidifying agent are the same as cement in soft soil, which includes hydrated calcium silicate (C-S-H) and ettringite (AFt). Furthermore, more C-S-H gel and AFt generated in the solidifying agent solidified soil than in the cement solidified soil. With the addition of 12% solidified materials (as shown in Fig. 8a and e), a very small amount of C-S-H gel formed on the surface of the soil particles. There are a large number of pores existed in the cement solidified soil. In addition, a very small amount of AFt is generated. When the same amount of the solidifying agent is incorporated (Fig. 8e), the soil particles are covered with a large amount of C-S-H, but smooth soil particles can still be observed. Similarly, a small amount of AFt is formed. With the addition of 15% solidified material (as shown in Fig. 8b and f), it can be seen that more C-S-H gels are formed in cement-solidified soil. The C-S-H gels are still separately distributed on soil particles. Instead, more AFt is generated in the solidifying agent solidified soil, and the soil particles are wrapped by a large amount of C-S-H gel. With the increasing amount of cement, more C-S-H gels are formed (Fig. 8c). The soil particles is cemented into a whole structure, and the compactness is significantly improved. A large amount of C-S-H gel is also generated in solidified soil, and a large amount of AFt generated and filled into the pores. The cementation and pores filling effectively improves the compactness of the solidified soil. The morphology shown in Fig. 8d and h is the solidified soil containing 21% solidified material. There is still a small amount of pores which can be found in cement solidified soil. The soil particles in the solidifying agent solidified soil have been completely covered and wrapped by C-S-H gel. The pores in organic clay are filled by massive AFt and C-S-H. There is no obvious boundary can be observed between the soil particles, and the solidifying agent solidified soil showed excellent entirety.

3.2.1.2. XRD test. The XRD test results of the solidified soil with different types of solidifying materials for curing 28 days are shown in Fig. 9. It can be found that when the 12% cement is added, the main characteristic peak in soft soil particles is SiO_2. There is a weak characteristic peak of C-S-H, which is caused by cement hydration. With the increase of cement content, the characteristic peak of $Ca(OH)_2$ appears in the XRD spectrum. When the content of solidifying materials is at a low level, the characteristic peak of the solidifying agent solidified soil is the same as that of cement solidified soil. After the addition of 15% solidifying agent, the weak characteristic peaks of C-S-H and AFt is generated. The peak intensity of AFt is obviously enhanced with the continuous increase of solidifying agent.

3.2.1.3. TG test. The mass loss in the range of 50–110 °C is from the loss of crystal water in AFt, as well as volatilization of natural water. The mass loss in the range of 400–520 °C is from the loss of crystal water in $Ca(OH)_2$ [30,31]. From the TG-DTA results shown in Fig. 10, it can be found that the cement stabilized soil and the solidifying agent stabilized soil both showed obvious mass loss at about 80 °C. Meanwhile, the DTA peak intensity of the solidifying agent stabilized soil is significantly higher than that of the cement stabilized soil. The peak intensity gradually enhances with the increase of the solidifying agent, which indicates that more AFt crystals are formed in the solidified soil. In addition, the cement-solidified soil has obvious mass loss at about 430 °C, and the DTA peak intensity gradually enhances with the increase of cement. Instead, the DTA peak do not appear in the solidified soil, indicating that more $Ca(OH)_2$ generate in the cement-solidified soil. The results of TG-DTA analysis are consistent with those of XRD.

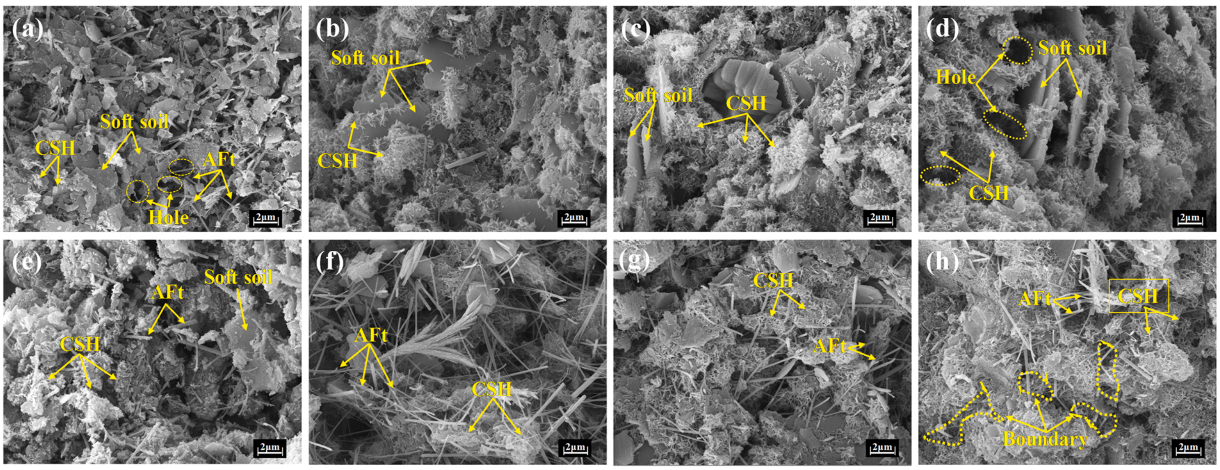

Fig. 8. Micro morphology of solidified soil with different types of solidifying materials, cement: (a) 12%, (b) 15%, (c) 18%, (d) 21%; solidifying agent: (e) 12%, (f) 15%, (g) 18% and (h) 21%.

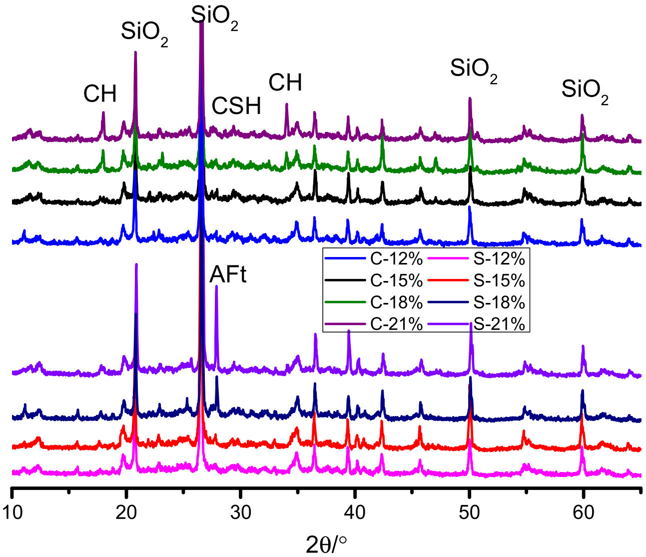

Fig. 9. XRD patterns of solidified soil with different types of solidified materials.

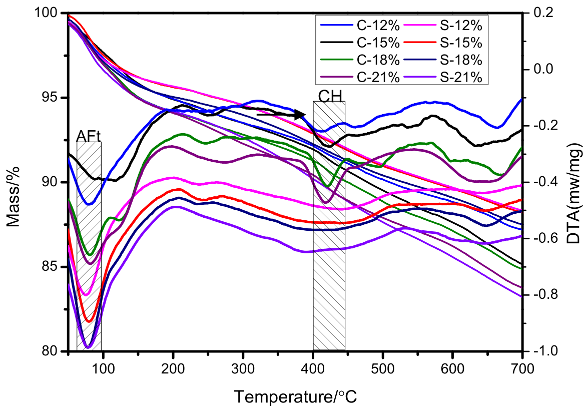

Fig. 10. TG test result of solidified soil with different types of solidified materials.

3.2.2. Solidification mechanism analysis

3.2.2.1. Alkali activation. The vitreous body in HCFA and SS is rapidly dissolved, and active components such as SiO_2 and Al_2O_3 are released as $[SiO_4]^{4-}$ and $[AlO_4]^{5-}$ when the pH is greater than 13.15 [32,33], and the chemical reaction is shown as follows (1) and (2). In view of this, this paper studied the effect of sodium sulfate on the pH of solidifying agent slurry, as shown in Fig. 11. The pH was always lower than 13 without the addition of Na_2SO_4. The pH of solidifying agent slurry after 30 min was 13.31 with the addition of 0.7% Na_2SO_4. The pH remained stable for a long time. Therefore, more active components are dissolved and polycondensated into a network structure in a short time, the chemical reaction is shown as follows (3) and (4). The result of Table 4 can be explained that sodium sulfate can rapidly stimulate the reactivity of HCFA and SS by increasing pH, while adding cement alone cannot have this effect.

$$-Si-O-Si-\xrightarrow{OH}[SiO_4]^{4-} \tag{1}$$

$$-Al-O-Al-\xrightarrow{OH}[AlO_4]^{5-} \tag{2}$$

$$Ca^{2+}+[SiO_4]^{4-}+(n-1)H_2O\xrightarrow{OH}CaO\cdot SiO_2\cdot nH_2O(C-S-H) \tag{3}$$

$$Ca^{2+}+[SiO_4]^{4-}+[AlO_4]^{5-}+mH_2O\xrightarrow{OH}3CaO\cdot Ai_2O_3\cdot 2SiO_2\cdot nH_2O(C-A-S-H) \tag{4}$$

Clay are potentially active. Clay minerals includes kaolinite, montmorillonite and illite. The Structural units are silicon oxygen

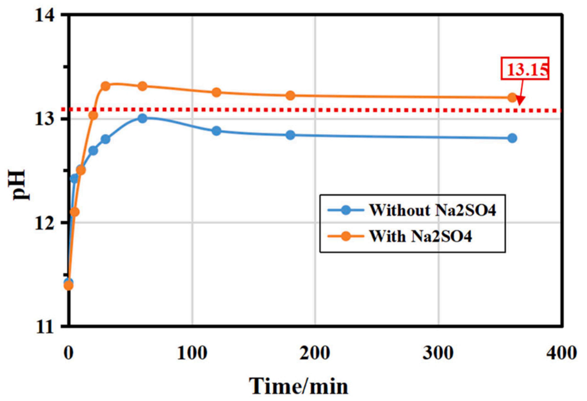

Fig. 11. Effect by product of sodium sulfate on pH of the multi-source solid waste solidifying agent slurry.

tetrahedron $[SiO_4]^{4-}$ and aluminum oxygen octahedron $[AlO_6]^{9-}$, which are connected by hydrogen bond and van der Waals force [34]. The secondary hydration can generate for the active oxides (such as silicon dioxide, aluminum oxide) in soil colloids under alkaline conditions and Ca^{2+}, S-C-H and S-A-H can thus be formed [35]. Similar to HCFA and SS, the increase of pH can promote the secondary reaction of soil. Therefore, the alkali activation of sodium sulfate may result in more active components of the clay participating in the secondary hydration reaction. Thus more S-C-H generated (as shown in Fig. 8), and the content of $Ca(OH)_2$ decreased (as shown in Fig. 10).

3.2.2.2. Dense packing. The pore diameter of cement solidified soil is distributed in 300–1000 nm, which is tens of times larger than that of cement concrete [29]. However, the quality of expansive materials, such as AFt in cement hydration products is strictly limited. So the cement solidified soil showed loose structure, and a large number of pores still existed (as shown in Fig. 8a, b, c and d SEM). $[AlO_4]^{5-}$ and C_3A were rapidly conversed into AFt after the addition of SO_4^{2-}, the chemical reaction is shown as follows (5) and (6). AFt increase the volume of solid phase by 120% [36], which could effectively fill the massive pores (300–1000 nm) in the solidified soil, as well as improve the compactness of the solidified soil. So the content of $Ca(OH)_2$ decreased, which is shown in TG results in Fig. 10. The content of AFt increased, which is shown in SEM and XRD results in Fig. 8 and Fig. 9.

$$[AlO_4]^{5-} + Ca^{2+} + SO_4^{2-} + OH^- \rightarrow 3CaO\cdot Al_2O_3\cdot 3CaSO_4.32\ H_2O\ (AFt) \quad (5)$$

$$C_3A + Ca^{2+} + SO_4^{2-} + OH^- \rightarrow 3CaO\cdot Al_2O_3\cdot 3CaSO_4.32\ H_2O\ (AFt) \quad (6)$$

The mechanical properties of solidified soil are significantly improved under the synergistic action of alkali activation and dense packing of Na_2SO_4.

3.3. Engineering application

3.3.1. Integrity of deep mixing pile

The cement mixing pile (80 kg/m cement) after 60 days of curing is shown in Fig. 12. It can be found from Fig. 12a that the integrity of cement mixing pile is poor. There are many broken piles can be found. The pile from the depth of 3–9 m exhibits a softened state, as well as low strength. Fig. 12b reveals that there are a lot of independent cement blocks in the broken cement mixing piles. The cement

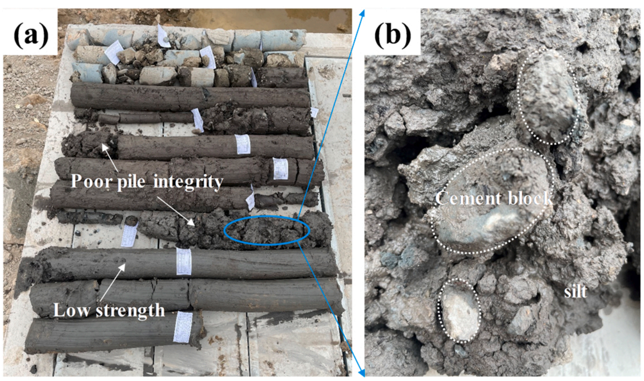

Fig. 12. Cement deep mixing pile (a) core sample and (b) poor integrity and homogeneity.

slurry has been injected to the organic clay, but which is not combined with the organic clay. The possible reason is that the cement slurry shows high viscosity, which make it difficult to fully penetrate into the deep organic clay geology, so the strength of the middle and lower parts of the cement deep mixing pile is low.

The solidifying agent deep mixing pile after the curing of 17d and 60d is shown in Fig. 13. It can be seen from Fig. 13a, b and c that in the initial stage of curing, the solidifying agent deep mixing pile shows excellent integrity. Even if the content of the solidifying agent is reduced to 50 kg/m, the integrity is still not weakened. Fig. 13d, e and f show that after a long-term curing time (60d), the solidifying agent deep mixing pile also exhibits excellent pile integrity.

3.3.2. Unconfined compressive strength

The early (14d curing age) and late (28d curing age) strengths of the solidifying agent deep mixing pile are tested, and the results are shown in Fig. 14. It can be found that with the addition of the solidifying agent, the pile strength gradually increases. The compressive strength of mixing pile with100kg/m solidifying agent after curing for 14d and 28d are 3.68 MPa and 4.33 MPa, respectively. When the content is reduced by 60% to 40 kg/m, the compressive strength of pile after the curing of 14d and 28d is 0.95 MPa and 2.77 MPa, respectively. Combined with Figs. 13 and 14, it can be concluded that the solidifying agent deep mixing pile shows excellent integrity, early strength and late strength.

The correlation between the strength of solidified soil in laboratory and the strength of deep mixing pile in field is shown in Fig. 15. It can be found that there is a positive linear correlation, that is, "$y = 0.832x + 0.1225$, $R^2 = 0.936$", which can be used to predict the UCS of the multi-source solid waste based solidifying agent deep mixing pile in the project.

4. Conclusion

In this paper, steel slag powder, high calcium fly ash and by-product Na_2SO_4 was utilized to develop a kind of low carbon emission soil solidifying material, and the solidification mechanism is studied. The solidifying agent is successfully applied to the deep mixing pile project. The main conclusions are as follows:

(1) The developed multi-source solid waste based solidifying agent showed excellent fluidity and satisfactory early strength for solidifying organic clay. The fluidity of the solidifying agent slurry is 170 mm (50 °C, 1 h), which is 55% higher than that of cement. The UCS of solidified soil at 28d curing age could be improved to 3.31 MPa with the addition of 15% solidifying agent.

(2) By product Na_2SO_4 showed double effect of alkali activation and dense packing. The pH of solidifying agent slurry was improved to 13.31 after the addition of 0.7% Na_2SO_4. Thus sodium sulfate could rapidly activate HCFA and SS to generate more C-S-H. The introduction of a large amount of SO_4^{2-} can react with $[AlO_4]^{5-}$, Ca^{2+}, OH^- to form AFt. Thus the amount of $Ca(OH)_2$ decreased gradually with the content of the solidifying agent. However, excessive addition of the solidifying agent will lead to excessive generation of AFt, which will lead to structural damage of solidified soil. Thus the optimum content of the solidifying agent in organic clay solidification is determined as about 27%.

(3) Organic clay cement deep mixing piles showed poor integrity and low strength. Solidifying agent deep mixing pile exhibited excellent pile integrity and satisfactory mechanical properties. With the addition of 65 kg/m solidifying agent, the early (14d) and late (28d) strengths of the deep mixing pile are improved to 2.04 MPa and 3.27 MPa, respectively. Solidifying agent deep mixing pile strength prediction for the project is proposed.

The reaction mechanism of active components in clay participating in secondary hydration under the action of the solidifying agent is still unknown. Therefore, further study will be conducted for the influence of by-product sodium sulfate on the secondary reaction of clay.

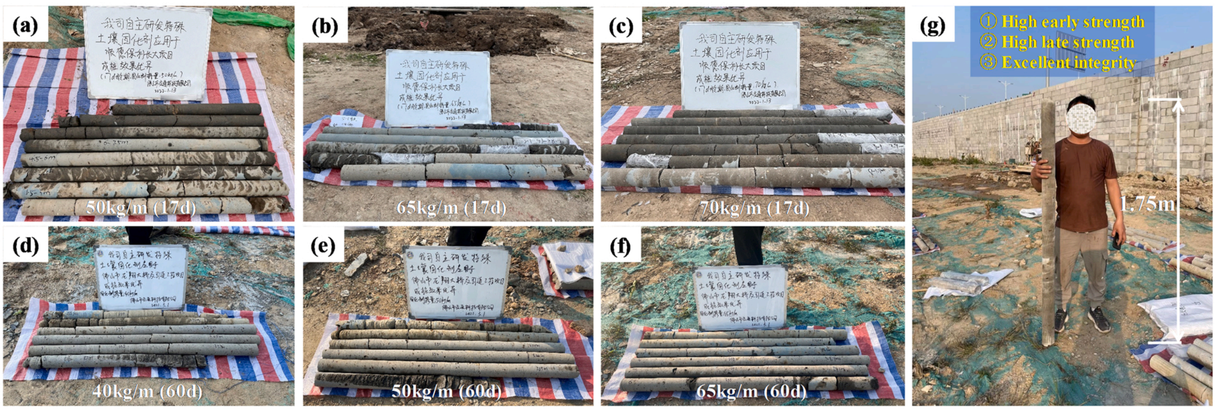

Fig. 13. Deep mixing pile with different content of the solidifying agent: (a), (b) and (c) is the application of the solidifying agent in Shunde District "robot valley" project; (d), (e), (f) and (g) is the application of the solidifying agent in "Longxiang bridge" project.

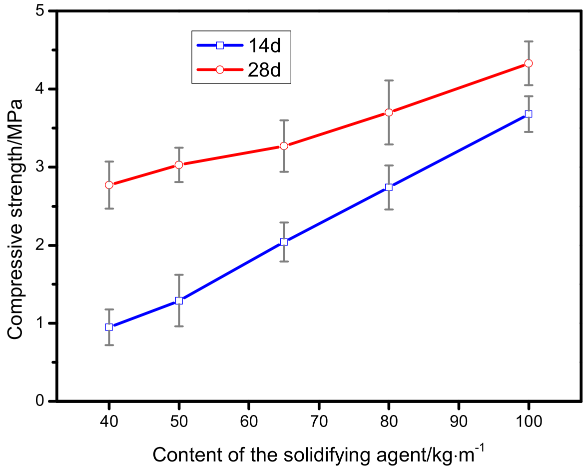

Fig. 14. Unconfined compressive strength of solidifying agent deep mixing pile at different curing period.

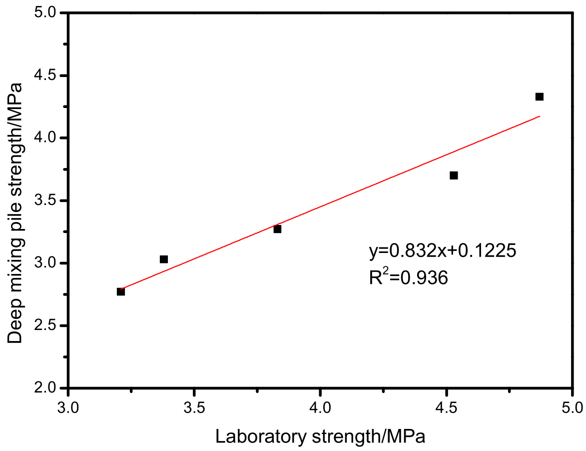

Fig. 15. Relationship between laboratory strength of solidifying agent solidified soil and the strength of solidifying agent deep mixing pile.

Declaration of Competing Interest

There are no conflicts of interest regarding the publication of this paper.

Data Availability

Data will be made available on request.

Acknowledgements

This research was funded by Foshan Self-Finance Science and Technology project (no. 2020001005441). Authors also thank the test support from the shiyanjia lab (www.shiyanjia.com).

References

[1] Y.D. Liao, X. Wang, L. Wang, et al., Effect of waste oyster shell powder content on properties of cement-metakaolin mortar, Case Stud. Constr. Mater. 16 (2022), e01088.
[2] T. Chompoorat, S. Likitlersuang, T. Thepumong, P. Jamsawang, P. Jongpradist, Solidification of sediments deposited in reservoirs with cement and fly ash for road construction, Int. J. Geosynth. Ground Eng. 7 (2021) 85.
[3] T. Chompoorat, S. Likitlersuang, S. Sitthiawiruth, et al., Mechanical properties and microstructures of stabilised dredged expansive soil from coal mine, Geomech. Eng. 25 (2) (2021) 143–157.
[4] B.A. Shu, M. Zhou, T.Y. Yang, et al., Performance study and engineering application of grouting materials with a large content of solid waste, Constr. Build. Mater. 312 (2021), 125464.

[5] T. Chompoorat, T. Thepumong, A. Khamplod, S. Likitlersuang, Mechanical microstructure properties and shrinkage characteristic of cement and fly ash treated soft Bangkok clay used for deep mixing, Constr. Build. Mater. 316 (2021), 125858.
[6] H.B. Wang, G.H. Sun, T. Sui, Landslide mechanism of waste rock dump on a soft gently dipping foundation: a case study in China, Environ. Earth Sci. 80 (5) (2021) 200.
[7] R. Ke, H.X. Wang, Y.Z. Tan, et al., Solidification of high organic matter content sludge by cement, lime and metakaolin, Period. Polytech. Civ. Eng. 63 (1) (2019) 53–62.
[8] C. Suksiripattanapong, T. Tesanasin, S. Tiyasangthong, et al., Use of cement and bottom ash in deep mixing application for stabilization of soft Bangkok clay, Arab. J. Sci. Eng. (2022).
[9] X.H. Lu, M.X. Cui, P.F. Wang, et al., Application in cement soil of stabilizer in silt soft soil of Wuxi in China, J. Coast. Res. 83 (2018) 316–323.
[10] H. Menaceur, O. Cuisinier, F. Masrouri, Impact of monotonic and cyclic suction variations on the thermal properties of a stabilized compacted silty soil, Transp. Geotech. 28 (2021), 100515.
[11] W. Tabyang, C. Suksiripattanapong, N. Wonglakorn, et al., Utilization of municipal solid waste incineration fly ash for non-bearing masonry units containing coconut fiber, J. Nat. Fibers (2022).
[12] L.U.D. Tambara, M. Taborda-Barraza, M. Cheriaf, et al., Effect of bottom ash waste on the rheology and durability of alkali activation pastes, Case Stud. Constr. Mater. 16 (2022), e00790.
[13] W. Tabyang, C. Suksiripattanapong, C. Phetchuay, et al., Evaluation of municipal solid waste incineration fly ash based geopolymer for stabilised recycled concrete aggregate as road material, Road. Mater. Pavement Des. 23 (9) (2022) 2178–2189.
[14] G.B. Zhang, Z.Q. Ding, R.H. Zhang, et al., Combined utilization of construction and demolition waste and propylene fiber in cement-stabilized soil, Buildings 12 (3) (2022) 350.
[15] W.Q. Lin, F.Y. Zhou, W.J. Luo, et al., Recycling the waste dolomite powder with excellent consolidation properties: Sample synthesis, mechanical evaluation, and consolidation mechanism analysis, Constr. Build. Mater. 290 (2021), 123198.
[16] C. Suksiripattanapong, R. Sakdinakorn, S. Tiyasangthong, et al., Properties of soft Bangkok clay stabilized with cement and fly ash geopolymer for deep mixing application, Case Stud. Constr. Mater. 16 (2022), e01081.
[17] L. Mengasini, M. Mavroulidou, M.J. Gunn, et al., Alkali-activated concrete mixes with ground granulated blast furnace slag and paper sludge ash in seawater environments, Sustain. Chem. Pharm. 20 (2021), 100380.
[18] Y.F. Deng, C.C. Xu, F. Marsheal, et al., Constituent effect on mechanical performance of crushed demolished construction waste/silt mixture, Constr. Build. Mater. 294 (2021), 123567.
[19] Benan Shu, Tengyu Yang, Yongling Li, et al., Effect of alkali-activated steel slag powder on solidification performance of silt soil, N. Build. Mater. 49 (03) (2022) 83–86 (in Chinese).
[20] A.R. Goodarzi, M. Movahedrad, Stabilization/solidification of zinc-contaminated kaolin clay using ground granulated blast-furnace slag and different types of activators, Appl. Geochem. 81 (2017) 155–165.
[21] J. He, X.K. Shi, Z.X. Li, et al., Strength properties of dredged soil at high water content treated with soda residue, carbide slag, and ground granulated blast furnace slag, Constr. Build. Mater. 242 (2020), 118126.
[22] P. Han, P.J. Han, Y.B. Yan, et al., Study on mechanical properties of acidic and alkaline silty soil by electrochemical impedance spectroscopy, Int. J. Electrochem. Sci. 13 (11) (2018) 10548–10563.
[23] S.H. Bahmani, N. Farzadnia, A. Asadi, et al., The effect of size and replacement content of nanosilica on strength development of cement treated residual soil, Constr. Build. Mater. 118 (2016) 294–306.
[24] Y. Jia, S.D. Hua, L.Y. Qian, et al., Development of steel slag-based solidification/stabilization materials for high moisture content soil, J. Renew. Mater. 10 (3) (2022) 735–749.
[25] Q.S. Chen, Y.B. Tao, Y. Feng, et al., Utilization of modified copper slag activated by Na2SO4 and CaO for unclassified lead/zinc mine tailings based cemented paste backfill, J. Environ. Manag. 290 (2021), 112608.
[26] Development trend analysis and investment prospect forecast report of China's synthetic fiber industry (2022–2029). 2021. (in Chinese) ⟨https://www.chyxx.com/industry/1109661.html⟩.
[27] S. Chatterjee, R. De, A. Gupta, Activated charcoal mediated purification of yellow sodium sulphate: a green process to utilize a hazardous by-product of the leather chemical industry, RSC Adv. 6 (59) (2016) 53651–53656.
[28] Jie Zhang. High-volume refined steel slag water-stabilized road base performance study. Guilin University of Technology. (Dissertation, in Chinese).
[29] Jun Wu, Li Liu, Yongfeng Deng, et al., Use of recycled gypsum in the cement-based stabilization of very soft clays and its micro-mechanism, J. Rock. Mech. Geotech. Eng. 14 (2022) 909–921.
[30] C.L. Oproiu, G. Voicu, A. Badanoiu, The solidification/stabilization of wastewater (From a Landfill Leachate) in specially designed binders based on coal ash, Materials 14 (19) (2021) 5610.
[31] E. Kapeluszna, W. Szudek, P. Wolka, et al., Implementation of alternative mineral additives in low-emission sustainable cement composites, Materials 14 (2021) 6423.
[32] Hui Liang. Study on the activity effect of fly ash. 2007. (Dissertation, in Chinese), DOI:⟨10.7666/d.y1116110⟩.
[33] Shouqing Liu, Zhongqiu Luo, Sen He, et al., Solidification/stabilization of calcium arsenate waste with blast furnace slag and fly ash geopolymer materials (in Chinese) (in Chinese), Chem. Ind. Eng. Prog. 36 (7) (2017) 2660–2666, https://doi.org/10.16085/j.issn.1000-6613.2016-2331.
[34] Ahmed Z. Khalifa, Özlem Cizer, Yiannis Pontikes, et al., Advances in alkali-activation of clay minerals, Cem. Concr. Res. 132 (2020), 106050.
[35] Yongfeng Deng, Li Liu, Yujun Cui, et al., Colloid effect on clogging mechanism of hydraulic reclamation mud improved by vacuum preloading, Can. Geotech. J. 56 (5) (2019) 611–620.
[36] Minqiang Jiang, Dingyi Yang, Resume of research progresses of ettringite in concrete (in Chinese) (in Chinese), Build. Tech. Dev. 31 (5) (2004) 132–135, https://doi.org/10.3969/j.issn.1001-523X.2004.05.058.